X-672-75-11

PREPRINT

NASA TM X- 70849

COPERNICUS OBSERVATIONS OF INTERSTELLAR ABSORPTION AT LYMAN ALPHA

(NASA-TM-X-70849) COPERNICUS OBSERVATIONS OF INTERSTELLAR ABSORPTION AT LYMAN ALPHA (NASA) 40 p HC $3.75 CSCL 03B

N75-19111

Unclas

G3/90 13280

RALPH C. BOHLIN

JANUARY 1975

GODDARD SPACE FLIGHT CENTER

GREENBELT, MARYLAND

For information concerning availability
of this document contact:

Technical Information Division, Code 250
Goddard Space Flight Center
Greenbelt, Maryland 20771

(Telephone 301-982-4488)

COPERNICUS OBSERVATIONS OF INTERSTELLAR ABSORPTION AT LYMAN ALPHA

Ralph C. Bohlin*

Goddard Space Flight Center

Greenbelt, Maryland 20771

Received January 6, 1975 by Ap.J.

* Guest Investigator with the Princeton University Telescope on the Copernicus Satellite, which is sponsored and operated by the National Aeronautics and Space Administration.

ABSTRACT

Column densities N_H of atomic hydrogen have been derived for 40 OB stars from spectral scans at Lα obtained by the Copernicus (OAO-3) satellite. The stars are all between 60 and 1100 pc away with a range of mean densities n_H of 0.01 to 2.5 atoms cm^{-3}. For 27 stars without significant amounts of molecular hydrogen, the mean gas to color-excess ratio is $\langle N_H/E(B-V) \rangle = 3.6 \times 10^{21}$ atoms cm^{-2} mag^{-1} and the mean density is $\langle n_H \rangle = 0.12$ atoms cm^{-3}. For 10 stars where the molecular hydrogen is at least 5 percent of the total hydrogen, $\langle N_H \text{ (total)}/E(B-V) \rangle$ is 5.4×10^{21} atoms cm^{-2} mag^{-1} and $\langle n_H \text{ (total)} \rangle$ is 0.7 atoms cm^{-3}. In this limited set of data, the gas to color-excess ratio in clouds varies from 1 to 3 times the mean outside of clouds. The presence of molecular hydrogen correlates with E(B-V), but the best tracer for H_2 is atomic hydrogen. The mean density of the gas for all 40 stars is much smaller than the mean of 0.7 atoms cm^{-3} obtained from 21-cm observations, because the brightest stars with less than average amounts of matter in the line of sight were selected for observation.

Subject headings: abundances - interstellar matter - spectra, ultraviolet

I. INTRODUCTION

The interstellar absorption line at Lα provides the best probe of the gas in the direction of early type stars. While the present Lα measurements extend to distances of only 1.1 kpc, the 21-cm emission measures include contributions from the entire line of sight through the galaxy and do not provide unambiguous information about the nearby gas, where differential galactic rotation is small. Measurements at 21-cm with the radio beam centered on the stars are consistent with the Lα data in the sense that emission from the gas beyond the stars increases the 21-cm value above the N_H from Lα, except in the case of δ Sco.

Savage and Jenkins (1972) and Jenkins and Savage (1974) used prototype spectra to obtain column densities for 95 stars using OAO-2 spectra at 12Å resolution. In a few cases, the mismatch between the prototype and the actual stellar spectrum seems to have caused Jenkins and Savage to overestimate the amount of gas. With the 0.2Å resolution of the U2 tube, the OAO-3 Copernicus spectra require no assumptions about the individual stellar spectra. However, the superposition of an offset, low resolution spectrum on the primary data complicated the analysis. An algorithm to subtract this stray light, as well as the scattered light from the grating, was developed and applied to the entire set of U2 scans. The column densities were deduced by multiplying the corrected data by exp (+τ), where τ is the optical depth for the damping profile and associated trial value for N_H.

The smaller values of N_H found by Copernicus for stars with little H_2 imply a lower $\langle N_H/E(B-V)\rangle$ than derived from OAO-2 data. The comparison of that ratio in and out of clouds provides no evidence for the depletion of atomic hydrogen in clouds, as suggested by Jenkins and Savage. The best estimate of the fundamental ratio $\langle N_H \text{ total})/E(B-V)\rangle$ is derived from stars with much H_2 in the line of sight and is in fortuitously good agreement with the OAO-2 result.

II. DATA ANALYSIS

The spectrometer on the Copernicus satellite (Rogerson et al., 1973a) contains four photomultiplier tubes mounted in pairs on two mobile carriages. The tubes designated V1 and V2 cover the near-ultraviolet between 1500 and 3200Å. The Lα region is scanned by the open window tubes U1 and U2 with 0.05 and 0.2Å slit widths, respectively Unfortunately, the U tubes have a vent hole that allows dispersed light at wavelengths longward of the exit slit to reach the photocathodes. Although the efficiency is low, the widths of these stray light holes are large enough to produce a significant signal. The U1 stray light (Rogers et al. 1973b) can be blocked by the dipping mirror on carriage-2, as the standard procedure. Because the Lα data are obtained most efficiently by U2, a comprehensive study was undertaken to devise an algorithm to compute the stray light, as well as the light scattered by the grating, for all U2 spectra.

a) Stray and scattered light

This discussion is intended to supplement and update the memo from D. G. York to users of Copernicus data on 26 March 1974. The responses for the Copernicus detectors are counts observed in the fixed 14 second integration time. The background counting rate of U2 caused by cosmic rays is generally between 20 and 60 counts outside of the South Atlantic anomaly, while the U1 background is a factor of 1.3 greater. The particle counts are subtracted from the raw data to produce U in the following discussion of stray and scattered light. To make further corrections, the wavelength coverage must be nearly complete over a

region of about 100Å or more, since both the stray and scattered light at one wavelength λ depend on properties of the spectrum at distant values of λ.

The observed spectrum $U(\lambda)$ is made up of the true spectrum $T(\lambda)$, the grating scatter $G(\lambda)$, and the stray light through the vent hole $S(\lambda)$,

$$U = T + G + S. \qquad (1)$$

The case of U1 data with the stray light hole blocked is particularly simple as $S_1 = 0$ and only the grating scatter need be specified in counts as

$$G_1(\lambda) = 0.02\ [U_1]\ (1200 \pm 200) + 0.067\ [U_1]\ (\lambda \pm 12), \qquad (2)$$

where the brackets indicate an average over the wavelength range in Angstroms specified in the following parentheses. Equation (2) is an approximation to the scattered light observed at the bottom of saturated interstellar lines in the U1 spectrum of τ Sco. The first term is a constant that depends only on the mean response to the star over the entire sensitive bandpass and the second term is the more important narrow angle scattering. Equation (2) produces a worst case error of two percent of the local continuum.

Similarly, the U2 scattered light is

$$G_2(\lambda) = 0.02\ [U_2-S_2]\ (1200 \pm 200) + 0.12\ [U_2-S_2]\ (\lambda \pm 12) \qquad (3)$$

The numerical constants need not be the same as for U1, because the geometry is different and a dipping mirror is present in the optical path. The constants were determined in conjunction with those in equations (5-7) to give the best solution.

A first approximation to the stray light S_2 was derived from a comparison of the U1 and U2 scans for τ Sco and ζ Oph with the stray-light hole blocked in U1. Trial and error resulted in improved constants that made the net signal approach zero for Lα and for some of the strongest bands of molecular hydrogen. The adopted approximation is

$$S_2(\lambda) = c(\lambda)\ [U_2 - S_2]\ (\lambda + \Delta\lambda \pm \delta\lambda), \tag{4}$$

where

$$\begin{aligned} c(\lambda) &= 5.82 \times 10^{-4}\ \lambda - 0.184 \quad \text{for } \lambda \leq 1207\text{Å} \\ &= 1.87 - 0.00112\ \lambda \quad \text{for } \lambda > 1207\text{Å}, \end{aligned} \tag{5}$$

$$\begin{aligned} \Delta\lambda &= 20 \quad \text{for } \lambda \leq 1079\text{Å} \\ &= 30.38 - 0.00962\lambda \quad \text{for } \lambda > 1079\text{Å}, \end{aligned} \tag{6}$$

and

$$\begin{aligned} \delta\lambda &= 2.0 \quad \text{for } \lambda \leq 1150\text{Å} \\ &= 3.5\ c(\lambda)/c(1216) \quad \text{for } \lambda > 1150\text{Å}. \end{aligned} \tag{7}$$

The stray light S_2 in equation (4) depends on the corrected spectrum $T_2 + G_2 = U_2 - S_2$ near the position of the stray light hole at $\Delta\lambda \sim 20$Å longward of the exit slit. The corrected spectrum is averaged over the bandpass $2\delta\lambda$ of the stray light hole, which is 4 to 7Å wide. The discontinuity in $\delta\lambda$ at 1150Å is an arbitrary choice that is compatible with the broader bandpass necessary near Lα and the narrower bandpass that helps in the difficult region of the Lyman bands of H_2. The solution is implemented

by approximating the correction for the spectrum in brackets in equation (4) at the longest wavelengths and then computing S_2 at successively shorter wavelengths. The complete solution for S_2 is used in equation (3) to compute the grating scatter. Since the expression (4) for S_2 converges rapidly, a satisfactory approximation for the longest $\Delta\lambda \sim 20\text{Å}$ of the scan is

$$S_2 = U_2(\lambda)/[1 + 1.25/c(\lambda - \Delta\lambda)]. \qquad (8)$$

The accuracy of the corrections for stray and scattered light in U2 can be estimated from the Lα line and other spectral features that have zero residual flux at line center. The errors are typically less than ± 5 percent of the continuum, although ± 10 percent deviations do occur. Random guidance errors are the dominant cause of these uncertainties. Any systematic errors in the correction technique are probably less than about 3 percent of the continuum. However, shortward of the lithium fluoride cutoff at $\sim 1050\text{Å}$, the stray light dominates and the errors increase rapidly. The original data, stray and scattered light, and corrected spectrum for ζ Oph observed 5-6 September 1972 appear in figure 1. Only the strong Lα line produces a significant dip in the scattered light. The stray light has pronounced features caused by the Lyman bands of H_2, CIII at 1176Å, Lα, and the P Cygni profile of NV near 1240Å, all shifted by Δλ with respect to the actual spectrum. The corrected spectrum has a counting rate near zero in the strong lines of the Lyman bands and at Lα.

b) Derivation of N_H

The column densities N_H to the stars were deduced from the reconstructions of the stellar spectra obtained by multiplying the observed data by exp $(+\tau)$, where the optical depth τ is computed for trial values of N_H and a pure damping line profile (Jenkins 1971, Bohlin 1973)

$$\tau(\lambda) = 4.26 \times 10^{-20} N_H / [6.04 \times 10^{-10} + (\lambda - \lambda_o)^2] . \qquad (9)$$

The wavelength at line center λ_o is 1215.67Å and the first term in the denominator is neglected. The interstellar absorption at Lα has a natural damping profile provided that the velocity dispersion of the gas is much less than the observed line width. For the smallest column density considered (5×10^{18} atoms cm^{-2}), the exponential absorption for a damping profile is 99 percent at 0.2Å or 50 km s^{-1} from line center. If a significant fraction of the gas has a radial velocity greater than $\pm$ 50 km s^{-1}, then the amount of gas will be less than that determined by assuming a damping profile. Since the instrumental resolution is 0.2Å, the center of the Lα line is always well resolved. A small adjustment to the zero level of the data is usually necessary to compensate the errors in the correction procedure of section II. a) and bring the Lα line to zero central flux.

Since the shape of the reconstructed spectrum in the neighborhood of $\tau = 1$ is quite sensitive to the choice of N_H, little judgment about the shape of the stellar spectrum is required and the uncertainty in the derived N_H is dominated by the photometric variability of the data. A comprehensive discussion of why the spectra of OB stars near Lα are well behaved is given by Jenkins (1970). Figures 2 and 3 show the corrected data and reconstructed spectra for four stars. The B1.5 IV star λ Sco has a Lα line with broad stellar wings

and a narrow core that is well resolved at 0.2Å resolution. With $N_H = 0.24 \times 10^{20}$ atoms cm^{-2}, the reconstruction turns up sharply between 0.5 and 1.0Å from line center, providing an upper limit for N_H. In HD28497, the Lα line has a damping profile with $N_H = 1.6 \times 10^{20}$. The upper and lower solid lines are reconstructions for N_H ± 20 percent and are the limits on the uncertainty of the measurement. Two earlier types with more interstellar absorption appear in figure 3. The reconstructions for δ Sco illustrate one of the worst problems with the photometric stability of the data. The left side of the line was scanned on one orbit and the right side on another, causing a small discontinuity in the scan near 1216Å. Because the corrections are all smooth functions, the discontinuity persists in the corrected data and is magnified by multiplying by exp (+τ). An uncertainty of about 20 percent is indicated by the good fit on the left for $1.2N_H$ and on the right for $0.8N_H$. Occasionally, the U_2 data have a smaller error limit as illustrated in figure 3 by the curves for τ CMa and N_H ± 10 percent.

For the three stars ζ Pup, ζ Oph, and τ Sco, column densities from U1 scans with the stray light blocked agree with N_H from the U2 spectra for the same star, but the accuracy is improved to 5 or 10 percent. For ζ Oph, two U2 spectra and the U1 spectrum are all in accord with $N_H = 5.4 \times 10^{20}$ ± 5 percent and with the value of 5.2×10^{20} quoted by Morton (1975), who used the same data. The interstellar absorption at Lβ was also studied in an attempt to verify and improve the results for Lα. Only the U1 spectrum of ζ Pup contained information at Lβ that permitted a straight forward confirmation of the Lα column density. The primary problem is that the Stark broadened stellar Lβ line is generally

much stronger than the interstellar component. For the largest column densities of HI, interstellar absorption in the (6,0) Lyman band of H_2 usually dominated the wings of Lβ.

Table 1 contains the results for the 40 stars. The spectral types, photometry, and intrinsic stellar properties are basically from the references used by Jenkins and Savage (1974), in order to make the results directly comparable. The error estimate is ± 20 percent unless noted by a percent error in parentheses following the column density.

III. PREVIOUS STUDIES OF Lα ABSORPTION

The Copernicus data provide the largest body of high precision spectra at Lα yet returned from above the earth's atmosphere. Pioneering flights by sounding rockets obtained valuable measurements, but the Lα spectra were few in number and of variable quality. The largest collection of hydrogen column densities comes from OAO-2, but the 12Å resolution of that spectrometer forced Savage and Jenkins (1972) to assume that all differences near Lα between stars of the same spectral class were caused by different amounts of interstellar absorption. Figure 4 compares the results of the two OAO satellites for the 31 stars in common. For 10 of the points that lie above the dashed line of perfect agreement, the respective error bars do not overlap and there is no value of N_H consistent with both determinations. Five of the ten cases of disagreement seem to be caused by a mismatch between the actual spectrum of the star and that of the protype spectrum assumed for the OAO-2 analysis. The five stars are λ Ori, ζ Per, γ Ara, HD28497, and ρ Leo. In all five spectra, the prototypes show some combination of weaker SiIII at 1206.5Å, weaker NV doublet near 1240Å, or a NV feature with less wavelength shift toward Lα. For example, HD28497 and its prototype λ Sco in figure 2 differ by about a factor of 2 in the strength of the SiIII line.

The other five cases of major disagreement are the points near the origin in figure 4 with arrows indicating upper limits that are more than a factor of three below the OAO-2 result. These stars are all B1 to B2 stars with N_H so low that the stellar Lα line is dominant. Fortunately, these stellar Lα lines have a narrow core compared to the flat interstellar profile. The positive count rate within 1Å of line center implies very low interstellar column densities. All five stars were identified by Savage

and Panek (1974) as having likely stellar contamination of the interstellar column densities derived from the OAO-2 survey. Savage and Panek based their conclusions on a comparison of OAO-2 data and unpublished stellar Lα profiles computed by Mihalas.

A few of the N_H values for B1 and later type stars in table 1 may still have a small amount of contamination from stellar Lα, if the measured profile is indistinguishable from a damping profile. For the low $N_H = 1.1 \times 10^{20}$ atoms cm^{-2}, both γ Peg and ζ Tau have a Lα line with an equivalent width of 7.7Å. Even if a line this weak is entirely stellar, an effective temperature over 25000°K for log g= 4.0 is necessary according to the Mihalas profiles (Savage and Panek 1974). An investigation of the stellar Lα lines is in progress. If that study produces a prediction for the amount of stellar contamination, a correction to the interstellar values will be published.

Except for the later spectral types, no systematic effect is evident in the differences between the 2 sets of OAO data as a function of spectral type. The Copernicus space densities n_H did <u>not</u> tend to increase in the later type stars as would be expected if stellar contamination were significant. The four stars in common with the Mariner 9 data of Bohlin (1973) differ by a maximum of 25 percent in the determination of N_H for the case of ε Per.

IV. COMPARISON WITH OTHER MEASUREMENTS

a) 21-cm

Grayzeck and Kerr (1974) have observed the 21-cm emission with a 21 arcmin beam centered on the star for one-half of the entries in table 1. Except for δ Sco, all of the 21-cm column densities are greater than the N_H from Lα, implying that much of the gas is behind the stars. In the Orion region where the stars are about 140 pc below the galactic plane, it is surprising that 90 percent of the gas often lies beyond the stars (cf. Jenkins 1970). Excluding the Orion stars, the correlation with the 21-cm measurements is still poor. Apparently, the distribution of the gas differs greatly from a plane parallel stratification, because the correction for the gas beyond the stars based on this model (Savage and Jenkins 1972) still does not significantly improve the agreement even for the specialized data considered here.

The 21-cm column density is less than the Lα value in the case of δ Sco. Smith (1973) obtained a kinetic temperature of about 50°K for the molecular hydrogen in front of δ Sco. A saturation of the 21-cm signal from a single cloud at 50°K is possible, but seems unlikely, because the high resolution data (0.34 km s^{-1}) have a peak brightness temperature near 50°K but show no individual feature with a width of 2 km s^{-1} that would be expected at 50°K. Perhaps, the brightness temperature is not constant over the 21 arcmin beam. A small inhomogeneity at the position of δ Sco could explain the higher value of N_H from Lα.

b) Molecular Hydrogen

Column densities $N(H_2)$ of molecular hydrogen have been measured for many of the stars in this survey by Spitzer, Drake, et al.(1973), Spitzer, Cochran, and Hirshfeld (1975), and Drake (personal communication). Smith (1973) obtained the value for δ Sco. The distribution of the measured column densities is illustrated in figure 5. No star has a column density $2N(H_2)$ between 10^{17} and 10^{19} atoms cm^{-2}. Most values of $2N(H_2)$ are less than 10^{17} atoms cm^{-2}, where the path to the stars is mainly through the intercloud medium. The few examples with $2N(H_2) > 10^{19}$ sample the dense interstellar clouds that always have at least 5 percent of the total gas in molecular form. The division of the data into two distinct groups motivates much of the following discussion. In all of the remaining figures, those stars with at least 5 percent H_2 are shown as open circles, while the filled circles represent the intercloud data with a negligible fraction of H_2.

c) Galactic Distribution

The mean space density n_H from the last column of table 1 is displayed in figure 6 as a function of galactic longitude ℓ^{II} for those stars with galactic latitude $|b^{II}| < 30°$. The open circles tend to lie above the filled circles, because a dense cloud in the line of sight will raise the mean density. The 11 stars in the direction of the galactic center with $310° \leq \ell^{II} \leq 10°$ suggest the presence of a dense, thin sheet of gas located about 160 pc away and extending over a large area of the sky. The stars closer than 160 pc have $N_H < \sim 10^{20}$ atoms cm^{-2}, and the stars between 170 and 1000 pc have N_H in the range 3 to 14 $\times$ 10^{20} atoms cm^{-2} and show no systematic increase with distance. The low density region with $n_H < \sim 0.2$ atoms cm^{-3} extends to greater distances toward decreasing ℓ^{II} through the position of the Gum Nebula, all the way out to $\sim$ 500 pc in Orion near $\ell^{II} = 200°$. Little H_2 is observed in this low density region.

Gott and Ostriker (1973) argue that the Gum Nebula is defined by the Hα emission and lies between $241° < \ell^{II} < 277°$, as indicated by the inner set of arrows under the words Gum Nebula in figure 6. The outer arrows locate the boundaries of the 90° nebula proposed by Alexander, et al. (1971) and Johnson (1973). Only θ Car lies in the extension towards greater ℓ^{II}, but seven stars are in the controversial region between $220° < \ell^{II} < 241°$ indicated by the vertical dashed lines in figure 6. Two stars β and ε CMa are about 200 pc away and have $n_H < 0.01$ atoms cm^{-3}, the lowest densities yet measured. The other 5 stars are about a kpc away suggesting that a very low density of neutral gas exists throughout this entire region all the way from the sun to more than twice the distance to the center of the Gum Nebula, located near γ^2 Vel and ζ Pup. An average

fractional ionization of 70 percent for the gas between the sun and the center of the Nebula is implied by the mean electron column density of 1.9×10^{20} electrons cm^{-2} derived from pulsar dispersion measures by Brandt, et al. 1971 and the mean N_H for ζ Pup and γ^2 Vel of 0.8×10^{20} atoms cm^{-2}.

d) Dust

The general correlation of gas and dust is illustrated in figure 7 showing N_H vs. the color excess E(B-V). The mean line is defined by the 27 stars that have negligible amounts of H_2 (filled circles) as $\langle N_H/E(B-V)\rangle = \Sigma N_H/\Sigma E(B-V) = 3.6 \times 10^{21}$ atoms cm^{-2} mag^{-1}, where each individual ratio is weighted by the respective E(B-V). The three Be or Bp stars are included, because their colors are reasonable. The seven upper limits on N_H are also included as actual measurements, because the values are so low that their exclusion would bias the answer upward. Pairs of open circles connected by a vertical line in figure 7 are the stars with large amounts of H_2. The lower circle is the column density in atomic form and the upper circle is the total hydrogen N_H (total) = $N_H + 2N(H_2)$. The Be star 59 Cyg has a measured fraction of 20 percent H_2 but is omitted, because the reddening is large and may be intrinsic.

In order to explore the correlation between gas and dust in more detail figure 8 was constructed. The mean gas and reddening per kpc weighted by the distance to each star were computed for the 27 intercloud stars as $\Sigma N_H/\Sigma r = 3.7 \times 10^{20}$ atoms cm^{-2} kpc^{-1} = 0.12 atoms cm^{-3} and $\Sigma E(B-V)/\Sigma r$ = 0.10 mag kpc^{-1}. The value of ΔN_H and $\Delta E(B-V)$ in figure 8 is the difference between the measurement and that expected over the distance r to each star. The dashed line is defined by the locus of points on the dashed line in figure 7 as $\Delta N_H/\Delta E(B-V) = \langle N_H/E(B-V)\rangle$. For stars with little H_2, the detailed correlation between the gas and dust indicates that these two components of the intercloud medium exist together in a universal ratio that is the same as that

determined by the mean 21-cm density of 0.7 atoms cm^{-3} and the mean reddening of 0.61 mag kpc^{-1} (Spitzer 1968). Some typical error bars in figure 8 show that τ Sco and κ Ori deviate from the dashed line by an amount that is significant, yet only about twice the expected error of $0.^{m}02$ in the photometry. Perhaps, the line of sight to these stars intercepts a diffuse cloud where the density is not enough for H_2 production.

For stars with much H_2, the lower open circles in figure 8 show more scatter about the mean than do the filled circles. Jenkins and Savage (1974) suggested that the atomic hydrogen is depleted in clouds by being converted to H_2. The evidence for this as a universal phenomenon is poor. Over half of the lower open circles lie above the mean line and only ϵ Per, α Cam, and ζ Oph have the expected total hydrogen (upper open circles). In all cases, the upper open circles lie above the dashed line with a range of total hydrogen $N_H + 2N(H_2)$ lying between 1 and 3 times the amount expected from the inter-cloud stars.

In figure 9, all the stars observed so far with $2N(H_2) > 10^{19}$ atoms cm^{-2} are separated from the stars with negligible H_2. The Be or Bp stars and the three nearest stars with E(B-V) = 0.02 to 0.03 are omitted because of the possible errors in the photometry. The dividing lines (dashed) fall near $E(B-V)/r = 0.3$ mag kpc^{-1} and an excess gas column density of $\Delta N_H = 2.4 \times 10^{20}$ atoms cm^{-2}. The best indicator for molecular hydrogen seems to be the atomic hydrogen with all the H_2 stars except ϵ Per having an atomic excess greater than 2.4×10^{20} atoms cm^{-2}. The presence of much H_2 in stars with low $\Delta E(B-V)$ in figure 8 and small E(B-V)/r in figure 9 suggests that

H_2 is formed somehow in gas phase reactions or, perhaps, these are old clouds that have lost their dust. More observations are needed to test the division of the open and filled circles of figure 9.

e) NaI, CaII, and KI

The values of N_H from Copernicus are compared with the visual interstellar lines that were observed with an interferomer and summarized by Hobbs (1974). Only 8 stars are common between the two surveys for KI and the correlation of N_H with N(CaII) shows the same large scatter found by Hobbs. The comparison of N_H with N(NaI) in figure 10 is somewhat different from the corresponding figure of Hobbs, who used OAO-2 values for N_H. Except for η CMa and π Sco, the points have reduced scatter about the dashed line drawn for N(NaI) proportional to N_H^2. Underhill and Fahey (1973) suggest that the NaI lines in η CMa are circumstellar. The addition of measured values for $2N(H_2)$ to the lower values for N_H (pairs of open circles) does not greatly affect the correlation. The slope of the dashed line confirms the results of Hobbs, but the NaI to HI ratios are higher. With the same constants for the ionization balance of sodium as Hobbs and the same n_e and N_H for his "standard cloud", the abundance of sodium relative to hydrogen is increased to 1.5×10^{-6} in agreement with the cosmic ratio of 1.7×10^{-6} (Withbroe 1971).

V. CONCLUSIONS

Because the sample of stars is not random, the mean density $\langle n_H \rangle$ cannot be derived by including the 27 intercloud stars that have little gas and dust. The means for the 10 stars with much H_2 are $\langle n_H \rangle$ = 0.47 atoms cm^{-3} and $\langle E(B-V)/r \rangle$ = 0.41 mag kpc^{-1}. Since these means are nearer to the commonly quoted averages of 0.7 atoms cm^{-3} and 0.61 mag kpc^{-1} for the medium as a whole, the total gas to dust for the 10 stars $\langle N_H \text{ (total)}/E(B-V) \rangle$ = 5.4 x 10^{21} atoms cm^{-2} mag^{-1} may be representative, despite the large scatter in the data. Multiplying by the mean reddening of 0.61 mag kpc^{-1} provides a best estimate of 1.1 atoms cm^{-3} for the mean density of the neutral atoms and molecules of hydrogen. Jenkins and Savage (1974) arrived at a similar value of 6.2 x 10^{21} atoms cm^{-2} mag^{-1} using a different data set and somewhat different logic. For HI only, Knapp and Kerr (1974) derived a gas to reddening ratio of 5.1 x 10^{21} atoms cm^{-2} mag^{-1} from 21-cm observations toward 81 globular clusters. Saturation should not be important, and corrections for any gas behind the clusters will probably not make their result compatible with the 3.6 x 10^{21} atoms cm^{-2} mag^{-1} found by Copernicus for atomic hydrogen alone. The larger gas to reddening ratio in clouds could be due to just a smaller mass fraction in grains or, possibly, a size or composition difference. Corrections for the ionized fraction of the gas will increase estimates of the gas to dust ratio more for intercloud data than for the cloud value since the H II regions represent a larger fraction of the distance to the closer group of stars. However, good support for the smaller gas to dust ratio comes from the ratio of the typical 21-cm density of 0.7 atoms cm^{-2} to the mean reddening of 0.61 mag kpc^{-1}, which gives 3.5 x 10^{21} atoms cm^{-2} mag^{-1}. Using X-Ray absorption measurements, Ryter,

Cesarsky, and Audouze (1975) find a ratio of equivalent hydrogen atoms to reddening of 6.8×10^{21} atoms cm^{-2} mag^{-1}, which includes atomic, molecular, and ionized hydrogen. A new survey in progress with J. Drake and B. Savage will greatly increase the number of stars observed with large fractions of H_2 and should enhance our understanding of the physical conditions associated with this common state of matter.

I wish to thank L. Spitzer and the entire Copernicus team at Princeton for sharing the data that was their reward for many years of work before the launch of OAO-3. E. Jenkins, B. Savage, and T. Stecher offered helpful advice and encouragement. D. York and T. Snow spent many hours of their time supervising the transfer of the data and providing orientation in the guest investigator program. Finally, I thank E. Greville and W. Budich for efficient processing of the spectra at GSFC.

Table 1
Results

HD	Name	Sp. T.	ℓ^{II}	b^{II}	V	B-V	E(B-V)	r	N_H	n_H
								pc	10^{20} cm^{-2}	cm^{-3}
886	γ Peg	B2 IV	109	-47	2.84	-.23	.01	167	1.1	.21
24398	ζ Per	B1 Ib	162	-17	2.85	+.12	.31	337	6.4(10)	.62
24760	ϵ Per	B0.5 III	157	-10	2.89	-.18	.10	287	2.5	.28
24912	ξ Per	O7.5	160	-13	4.04	+.02	.34	457	13	.92
28497		B1.5 Ve	209	-37	5.59	-.24	.01	527	1.6	.098
30614	α Cam	O9.5 Ia	144	14	4.29	+.03	.30	828	8.0	.31
36486	δ Ori	O9.5 II-III	204	-18	2.24	-.22	.08	319	1.7	.17
36861	λ Ori	O8	195	-12	3.39	-.19	.12	443	6(25)	.44
37043	ι Ori	O9 III	210	-20	2.77	-.24	.07	449	1.4(15)	.10
37128	ϵ Ori	B0 Ia	205	-17	1.69	-.18	.06	348	2.8	.26
37202	ζ Tau	B2 IVp*	186	-6	3.03	-.19	.05	172	1.1	.21
37742	ζ Ori	O9.5 Ib	206	-17	1.77	-.21	.06	322	2.6	.26
38666	μ Col	O9.5 IV	237	-27	5.16	-.29	.01	1086	0.70	.021
38771	κ Ori	B0.5 Ia	215	-19	2.05	-.18	.04	463	3.3(10)	.23
40111	139 Tau	B1 Ib	184	1	4.82	-.06	.13	1061	8.0	.24
44743	β CMa	B1 II-III	226	-14	1.97	-.24	.01	213	<0.05	<.008
47839	15 Mon	O7	203	2	4.66	-.24	.08	899	2.5	.09
52089	ϵ CMa	B2 II	240	-11	1.50	-.21	.01	179	<0.05	<.009
53138	σ^2 CMa	B3 Ia	236	-8	3.01	-.08	.05	855	1.5	.057
57060	29 CMa	O7 f	238	-5	4.95	-.15	.17	908	5.0	.18
57061	τ CMa	O9 Ib	238	-6	4.40	-.15	.13	1052	5.0(10)	.15
58350	η CMa	B5 Ia	243	-6	2.44	-.09	.00	773	0.70	.029
66811	ζ Pup	O5 f	256	-5	2.25	-.27	.05	380	0.97(5)	.083
68273	γ^2 Vel	WC8 + O9I	263	-8	1.83	-.25		380†	0.60(10)	.051
91316	ρ Leo	B1 Iab	235	53	3.85	-.14	.05	955	1.8	.061
93030	θ Car	B0.5 Vp	290	-5	2.76	-.22	.06	207	1.9	.30
116658	α Vir	B1 IV	316	51	0.97	-.23	.03	99	<0.1	<.033
121263	ζ Cen	B2.5 IV	314	14	2.55	-.22	.00	123	1.05	.28
122451	β Cen	B1 III	312	1	0.61	-.25	.01	99	0.33(10)	.11
143018	π Sco	B1 V + B2	347	20	2.91	-.20	.05	219	5.2(10)	.77
143275	δ Sco	B0.5 IV	350	23	2.32	-.12	.16	181	14	2.5
149038	μ Nor	B0 Ia	339	3	4.92	+.13	.37	1004	10	.32
149438	τ Sco	B0 V	352	13	2.81	-.25	.05	258	3.1(10)	.39
149757	ζ Oph	O9.5 Vnn	6	24	2.56	+.02	.32	173	5.2(5)	.97
157246	γ Ara	B1 Ib	335	-11	3.33	-.14	.05	597	4.8	.26
158408	υ Sco	B2 IV	351	-2	2.68	-.23	.01	155	<0.18	<.038
158926	λ Sco	B1.5 IV	352	-2	1.63	-.22	.03	112	<0.24	<.07
175191	σ Sgr	B3 IV	10	-12	2.03	-.22	.00	80	<0.30	<.12
193924	α Pav	B2.5 V	341	-35	1.94	-.20	.02	63	<0.20	<.10
200120	59 Cyg	B1.5 Venn	88	1	4.75	-.04	.21	272	1.8	.21

*Hoffleit (1964)
†Distance for γ^2 Vel set equal to that for ζ Pup.

REFERENCES

Alexander, J. K., Brandt, J. C., Maran, S. P., and Stecher, T. P. 1971, Ap. J., 167, 487.

Bohlin, R. C. 1973, Ap. J., 182, 139.

Brandt, J. C., Stecher, T. P., Crawford, D. L., and Maran, S. P. 1971, Ap. J. (Letters), 163, L99.

Gott, J. R., and Ostriker, J. P. 1973, in The Gum Nebula and Related Problems, ed. S. P. Maran, J. C. Brandt, and T. P. Stecher, NASA SP-332, 42.

Grayzeck, E. J., and Kerr. F. J. 1974, A.J., 79, 368.

Knapp, G. R., and Kerr, F. J. 1974, Astr. and Ap., 35, 361.

Hobbs, L. M. 1974, Ap. J., 191. 381.

Hoffleit, D. 1964, Catalogue of Bright Stars (Yale University Observatory).

Jenkins, E. B. 1970, in Ultraviolet Stellar Spectra and Related Ground-Based Observations (IAU Symp. No. 36), ed. L. Houziaux and H. E. Butler (Dordrecht, D. Reidel Publishing Co.) p. 281.

Jenkins, E. B. 1971, Ap. J., 169, 25.

Jenkins, E. B., and Savage, B. D. 1974, Ap. J., 187, 243.

Johnson, H. M. 1973, in The Gum Nebula and Related Problems, ed. S. P. Maran, J. C. Brandt, and T. P. Stecher, NASA SP-332, 12.

Morton, D. C. 1975, Ap. J., in press.

Rogerson, J. B., Spitzer, L., Drake, J. F., Dressler, K., Jenkins, E. B., Morton, D. C., and York, D. G. 1973a, Ap. J. (Letters), 181, L97.

Rogerson, J. B., York, D. G., Drake, J. F., Jenkins, E. B., Morton, D. C., and Spitzer, L. 1973b, Ap. J. (Letters), 181, L110.

Ryter, C., Cesarsky, C. J., and Audouze, J. 1975, Ap. J., in press.

Savage, B. D., and Jenkins, E. B. 1972, Ap. J., 172, 491.

Savage, B. D., and Panek, R. J. 1974, Ap. J., 191, 659.

Smith, A. M. 1973, Ap. J. (Letters), 179, L11.

Spitzer, L. 1968, Diffuse Matter in Space, (New York, John Wiley & Sons).

Spitzer, L., Cochran, W. D., and Hirshfeld, A. 1975, Ap. J. Suppl., No. 266.

Spitzer, L., Drake, J. F., Jenkins, E. B., Morton, D. C., Rogerson, J. B., and York, D. G. 1973, Ap. J. (Letters), 181, L116.

Underhill, A. B., and Fahey, R. P. 1973, Ap. J. Suppl., 25, 463.

Withbroe, G. L. 1971, The Menzel Symposium (NBS Special Pub. 353), ed. K. B. Gebbie (Washington: U. S. Government Printing Office).

FIGURE CAPTIONS

Figure 1. U2 data for ζ Oph. Upper: Observed response U_2. Center: The solid line is the stray light S_2 and the dashed line is the computed grating scatter G_2. Lower: Corrected spectrum T_2.

Figure 2. Dashed lines are corrected spectra with the center of the Lα line at zero residual flux. The solid lines are reconstructions of the stellar spectra using a damping profile for the interstellar absorption and the value for N_H listed below the star name and spectral type. For λ Sco the solid line is an upper limit to N_H. In the lower half, the reconstructions are for the final value of N_H and the error limits of ± 20 percent. Wavelengths are in the frame of the most prominent interstellar cloud in the visual.

Figure 3. Corrected data and reconstructions as in figure 2. For δ Sco the error limits on N_H are ± 20 percent and for τ CMa ± 10 percent.

Figure 4. Comparison of values for N_H from the OAO-2 data reduced by Savage and Jenkins (1972) and Jenkins and Savage (1974) with the OAO-3 results. The dashed line at 45° represents perfect agreement.

Figure 5. Distribution of measured column densities of molecular hydrogen. No values of $2N(H_2)$ lie between 10^{17} and 10^{19} atoms cm^{-2}.

Figure 6. Mean space densities n_H vs. galactic longitude ℓ^{II} for stars with $|b^{II}| < 30°$. Arrows indicate upper limits.

Figure 7. Relation between the gas N_H and dust measured by the color excess E(B-V). The dashed line has a slope of 3.6×10^{21} atoms cm^{-2} mag^{-1}. Open circles are stars with more than 5 percent molecular hydrogen. The lower open circle of the pairs connected by vertical lines is the atomic hydrogen, while the upper circle is the total $N_H + 2N(H_2)$. For π Sco, $2N(H_2)$ is greater than 10^{19} atoms cm^{-2}, but the precise value is unavailable.

Figure 8. Deviations of N_H and E(B-V) from the mean values expected over the distance to the stars. The dashed line and pairs of open circles are the same as in figure 7.

Figure 9. Separation of cloud and intercloud data. Pairs of open circles are the same as in figure 7. The dashed lines at $\Delta N_H = 2.4 \times 10^{20}$ atoms cm^{-2} and $E(B-V)/r = 0.3$ mag kpc^{-1} define a region containing all the stars with little H_2. Note the large scatter of the points about the mean reddening of 0.61 mag kpc^{-1}.

Figure 10. Comparison of sodium to hydrogen similar to figure 5b of Hobbs (1974). Filled and open circles are defined in figure 7.

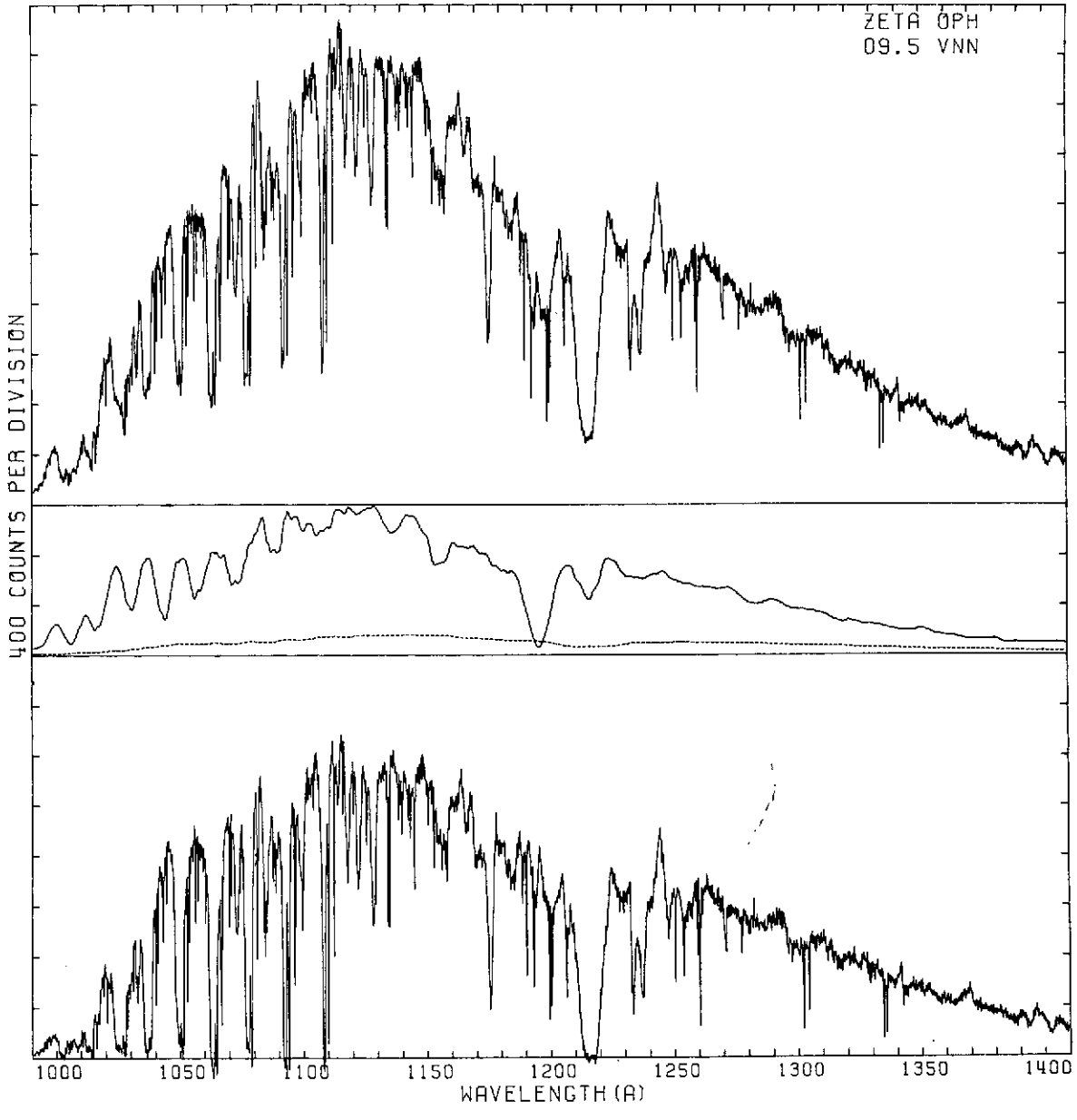

FIG. 1

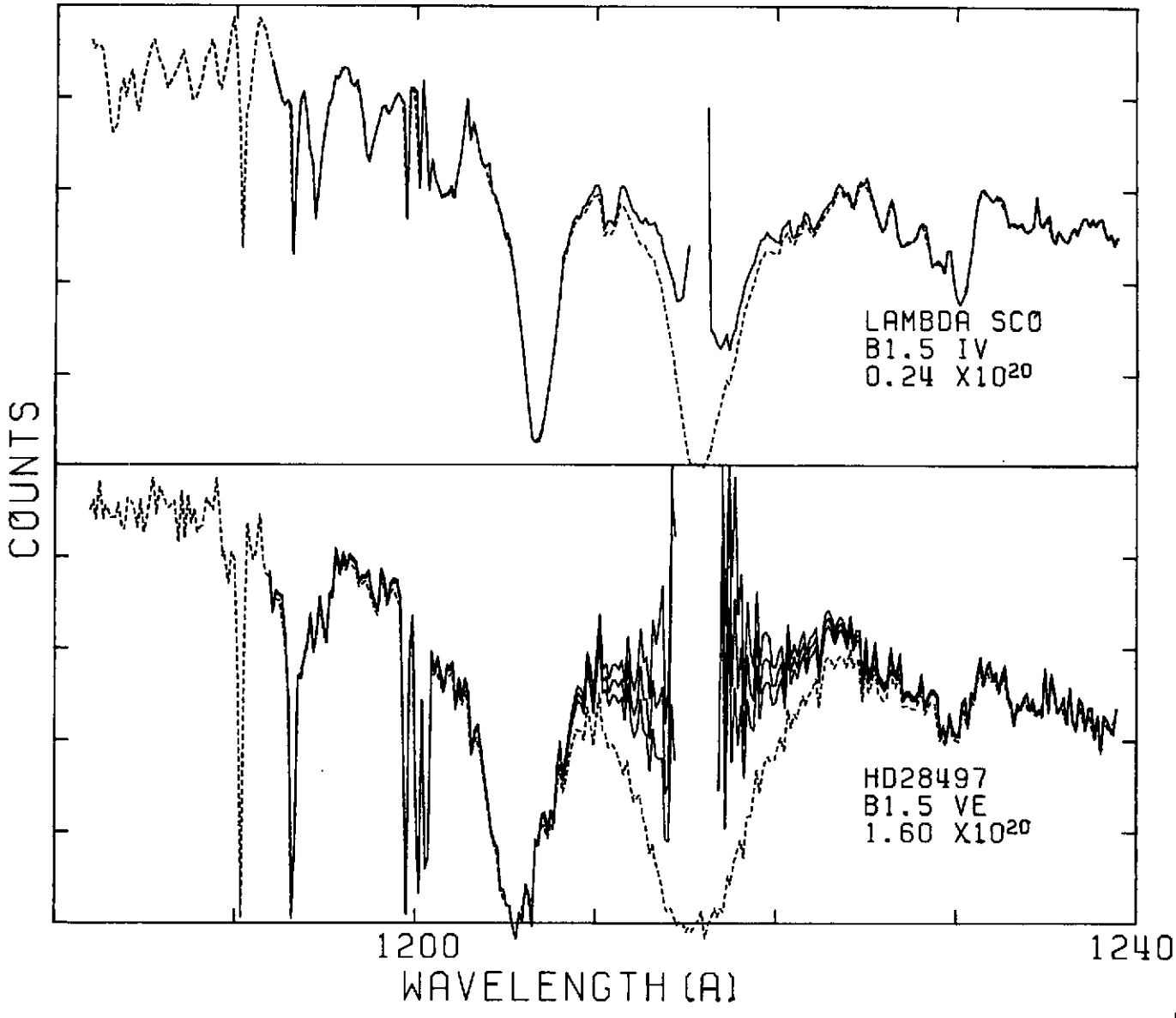
LAMBDA SCO
B1.5 IV
0.24 X10^20
HD28497
B1.5 VE
1.60 X10^20
COUNTS
1200
1240
WAVELENGTH (A)

FIG. 2

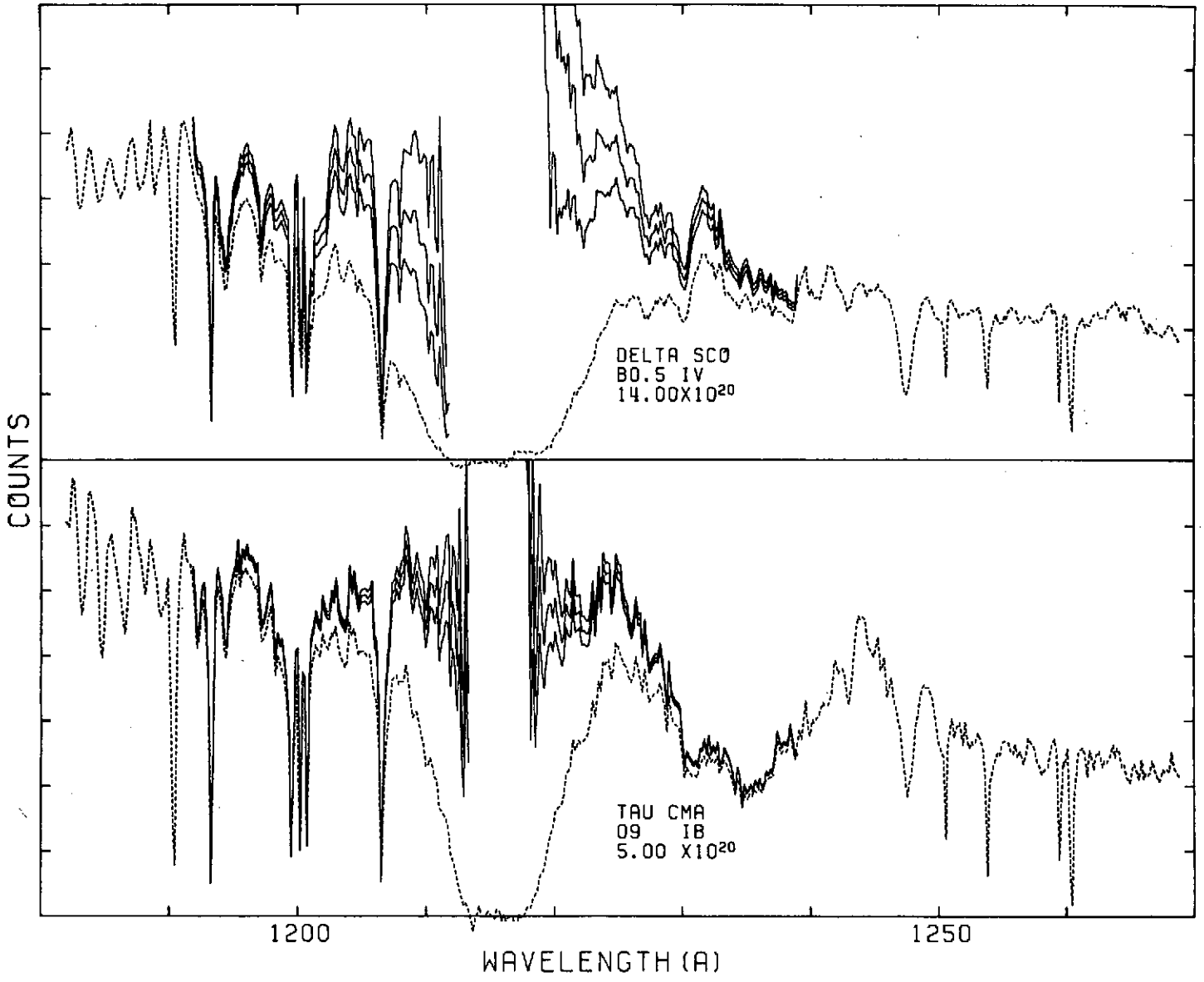

FIG. 3

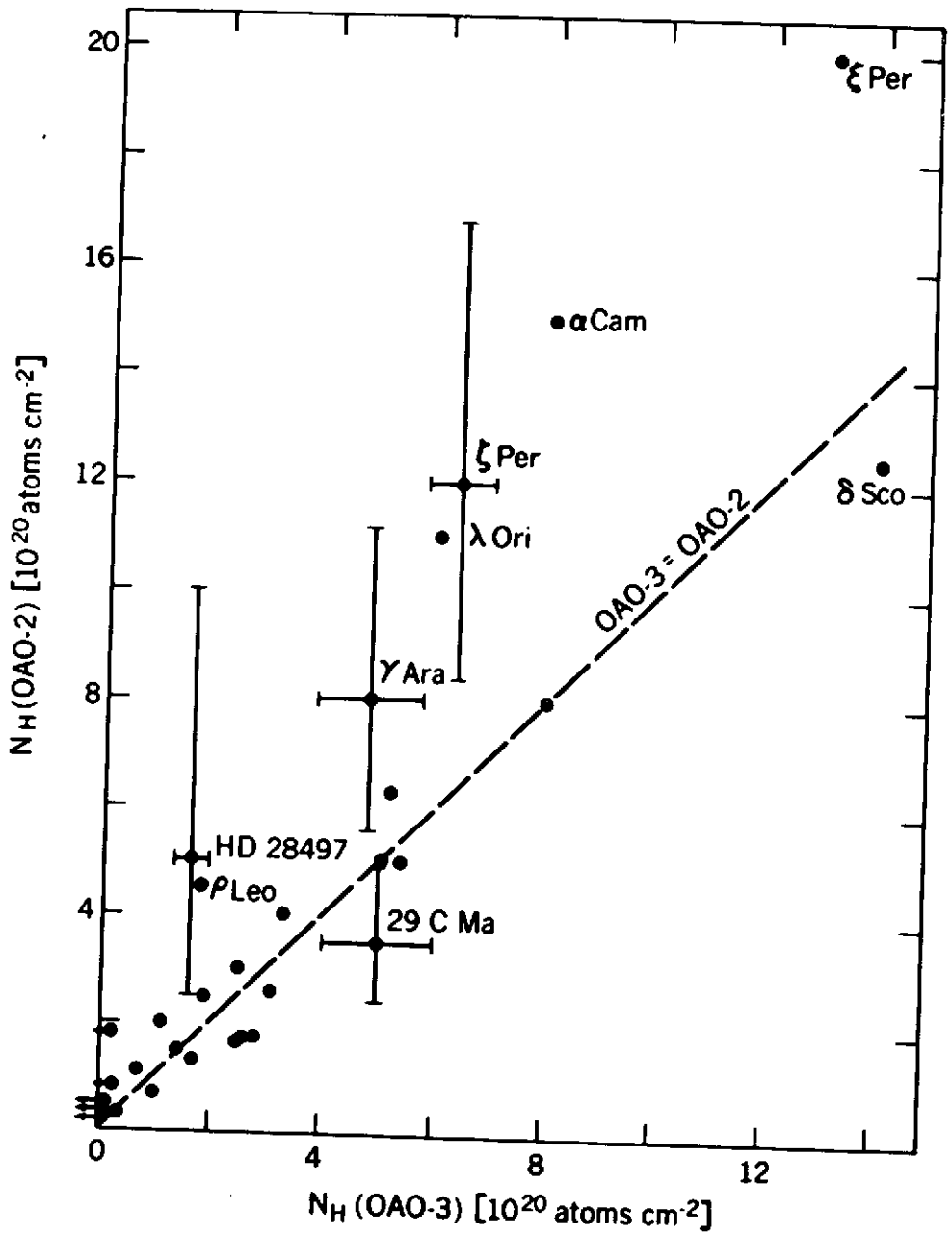
20
16
12
8
4
0
4
8
12
N_H(OAO-2) [10^{20} atoms cm^{-2}]
N_H (OAO-3) [10^{20} atoms cm^{-2}]
ξ Per
αCam
ζ Per
λ Ori
δ Sco
γ Ara
OAO-3 = OAO-2
HD 28497
ρ Leo
29 C Ma

FIG. 4

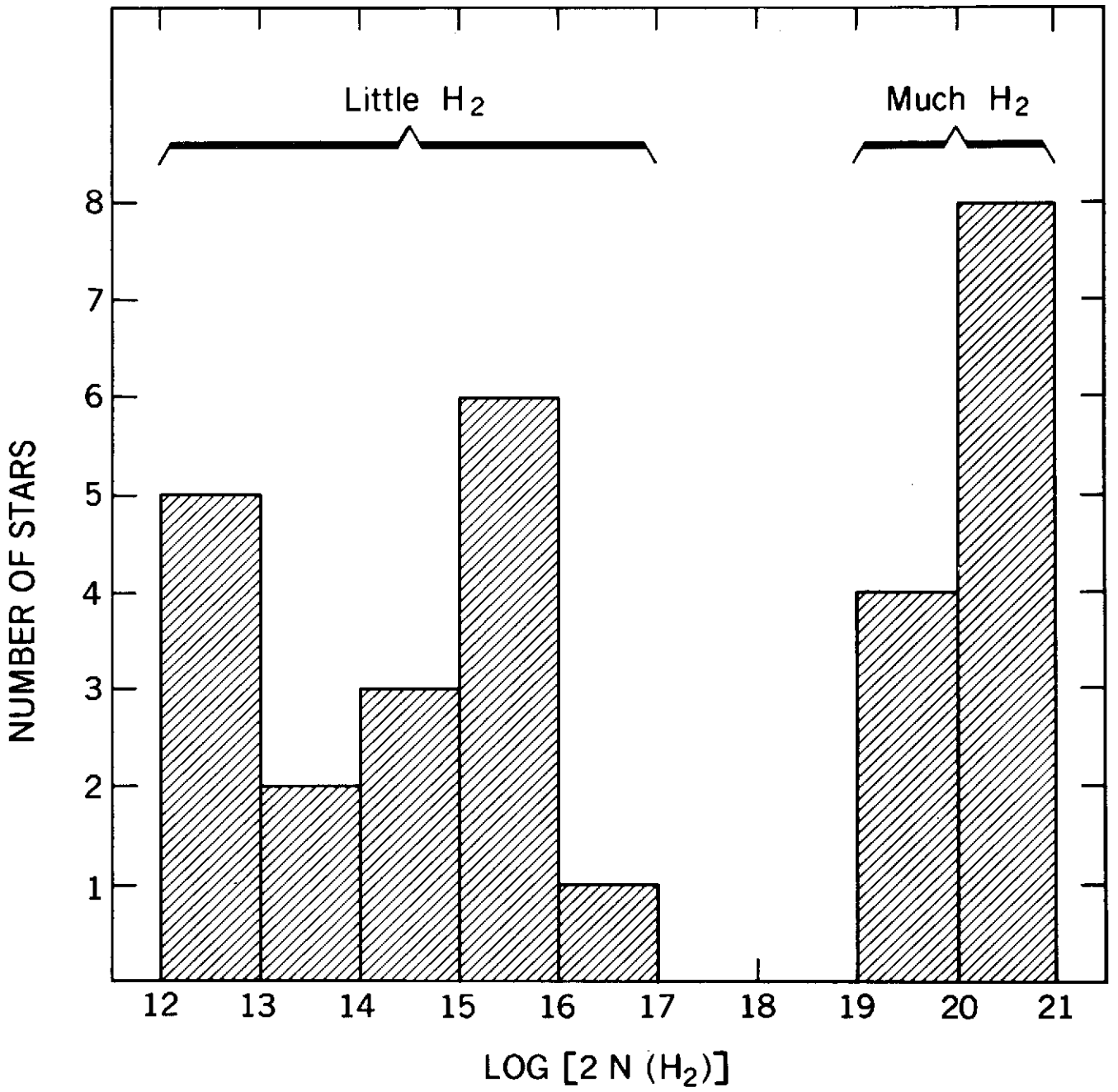

FIG. 5

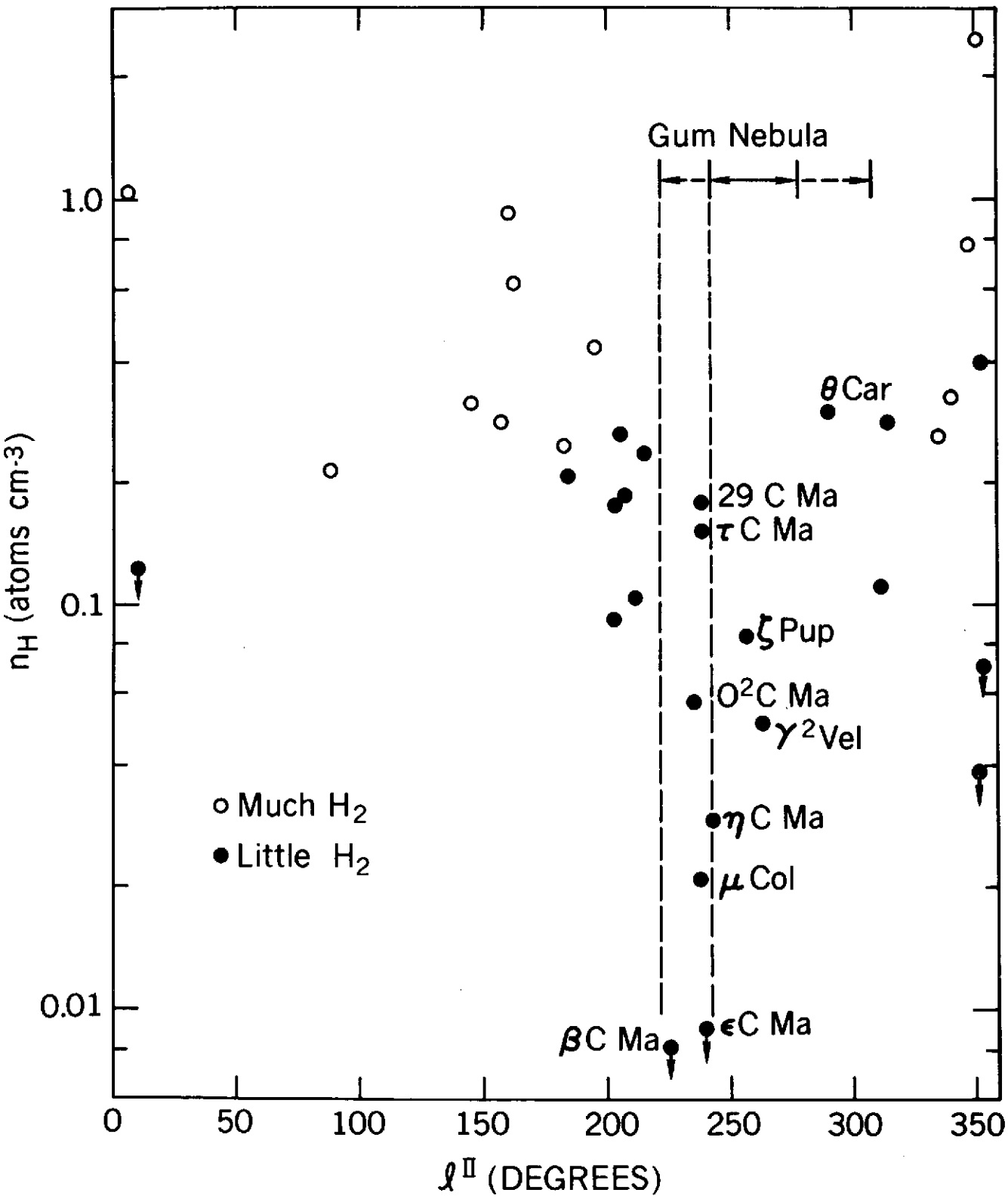
Gum Nebula
1.0
0.1
0.01
n_H (atoms cm^{-3})
θ Car
29 C Ma
τ C Ma
ζ Pup
O^{2}C Ma
γ^2 Vel
η C Ma
μ Col
βC Ma
εC Ma
Much H_2
Little H_2
0
50
100
150
200
250
300
350
l^{II} (DEGREES)

FIG. 6

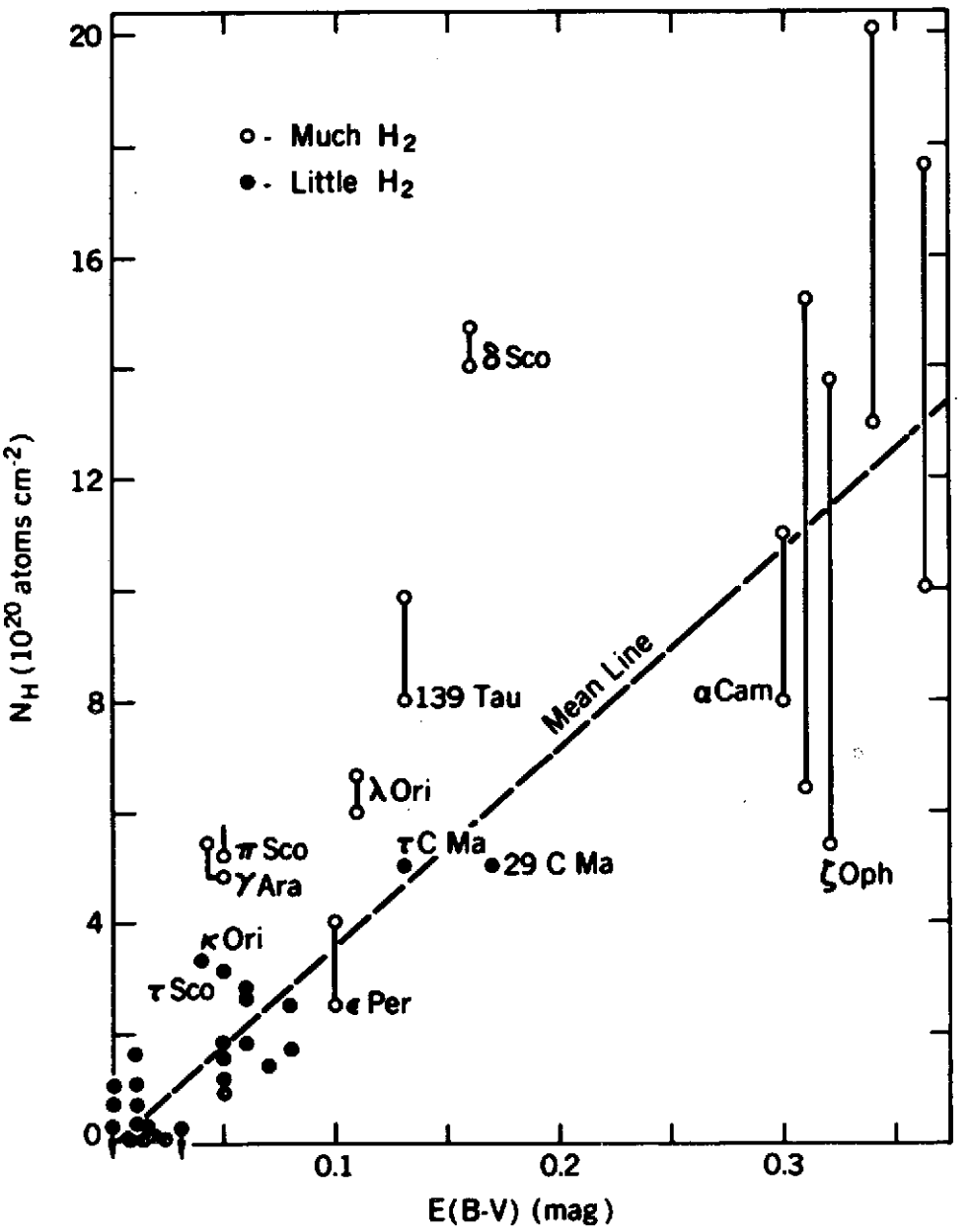
20
16
12
8
4
0
0.1
0.2
0.3
E(B-V) (mag)
N_H (10^{20} atoms cm^{-2})
o - Much H_2
● - Little H_2
δ Sco
139 Tau
λ Ori
π Sco
γ Ara
τ C Ma
29 C Ma
κ Ori
τ Sco
ε Per
Mean Line
α Cam
ζ Oph

FIG. 7

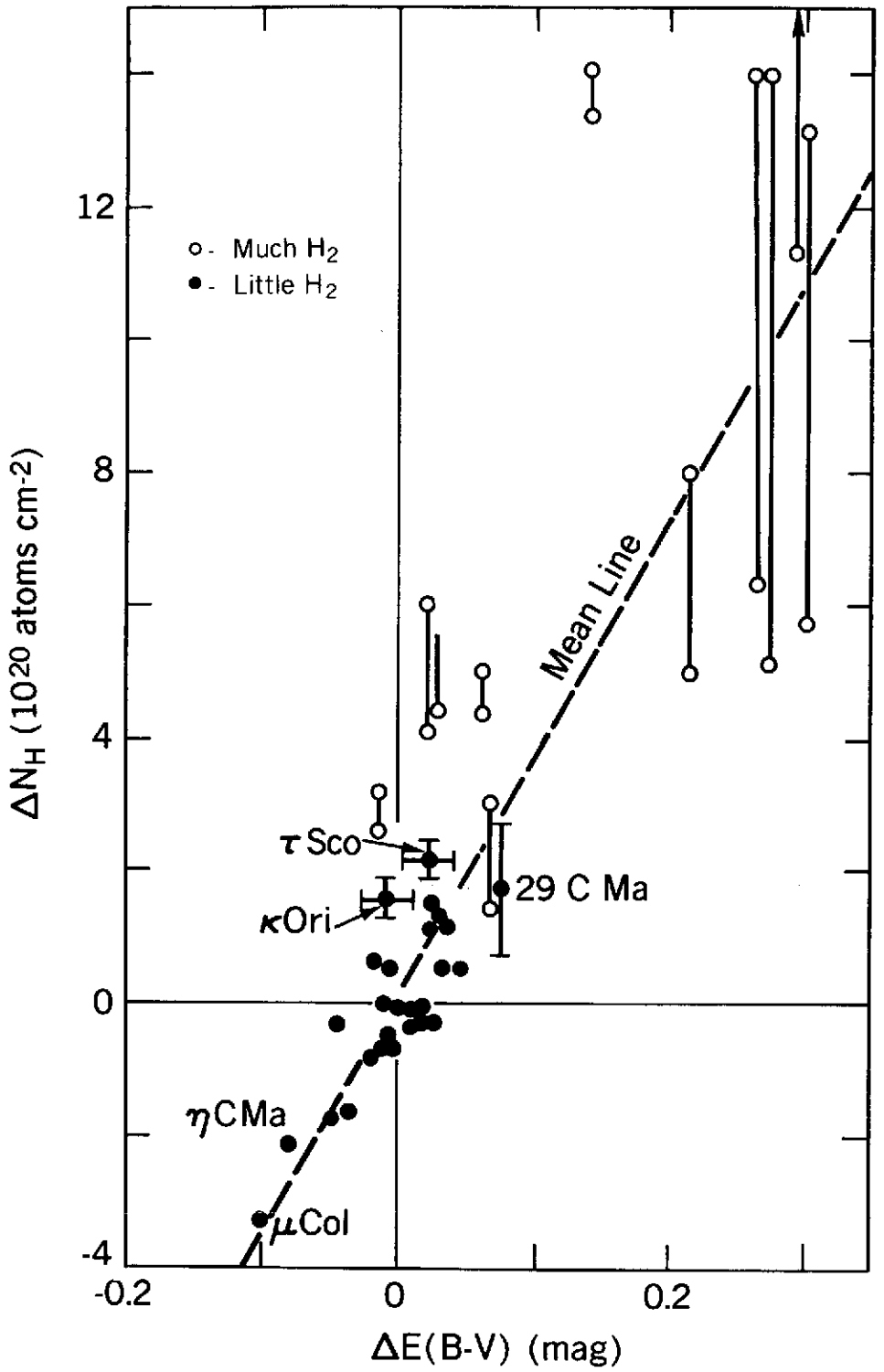
12
8
4
0
-4
-0.2
0
0.2
ΔE(B-V) (mag)
ΔN_H (10^20 atoms cm^-2)
o - Much H2
• - Little H2
Mean Line
τ Sco
κ Ori
29 C Ma
η C Ma
μ Col

FIG. 8

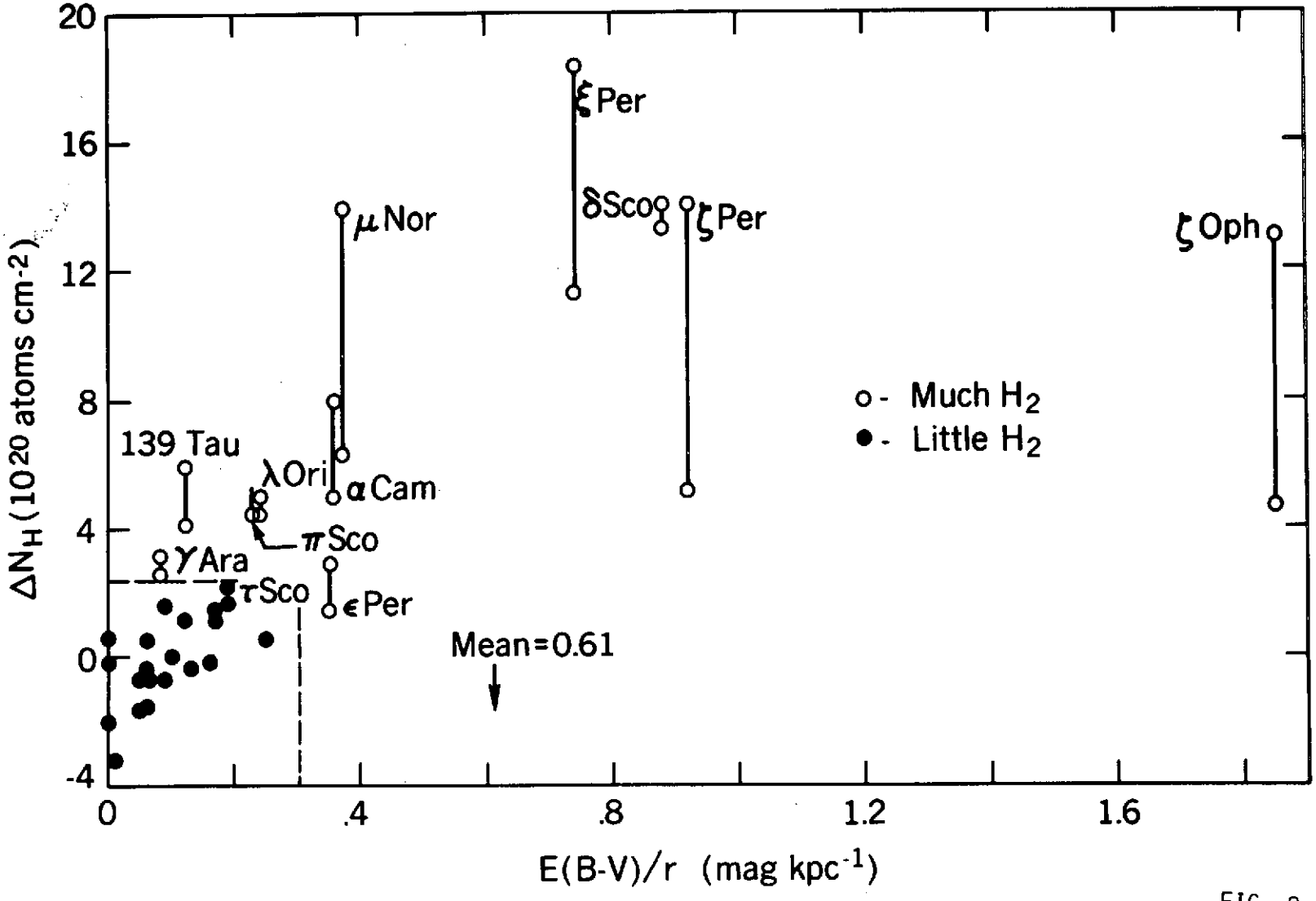
20
16
12
8
4
0
-4
0
.4
.8
1.2
1.6
ΔN_H (10^20 atoms cm^-2)
E(B-V)/r (mag kpc^-1)
ξ Per
δ Sco
ζ Per
μ Nor
ζ Oph
139 Tau
λ Ori
α Cam
π Sco
γ Ara
τ Sco
ε Per
Mean=0.61
o - Much H2
● - Little H2

FIG. 9

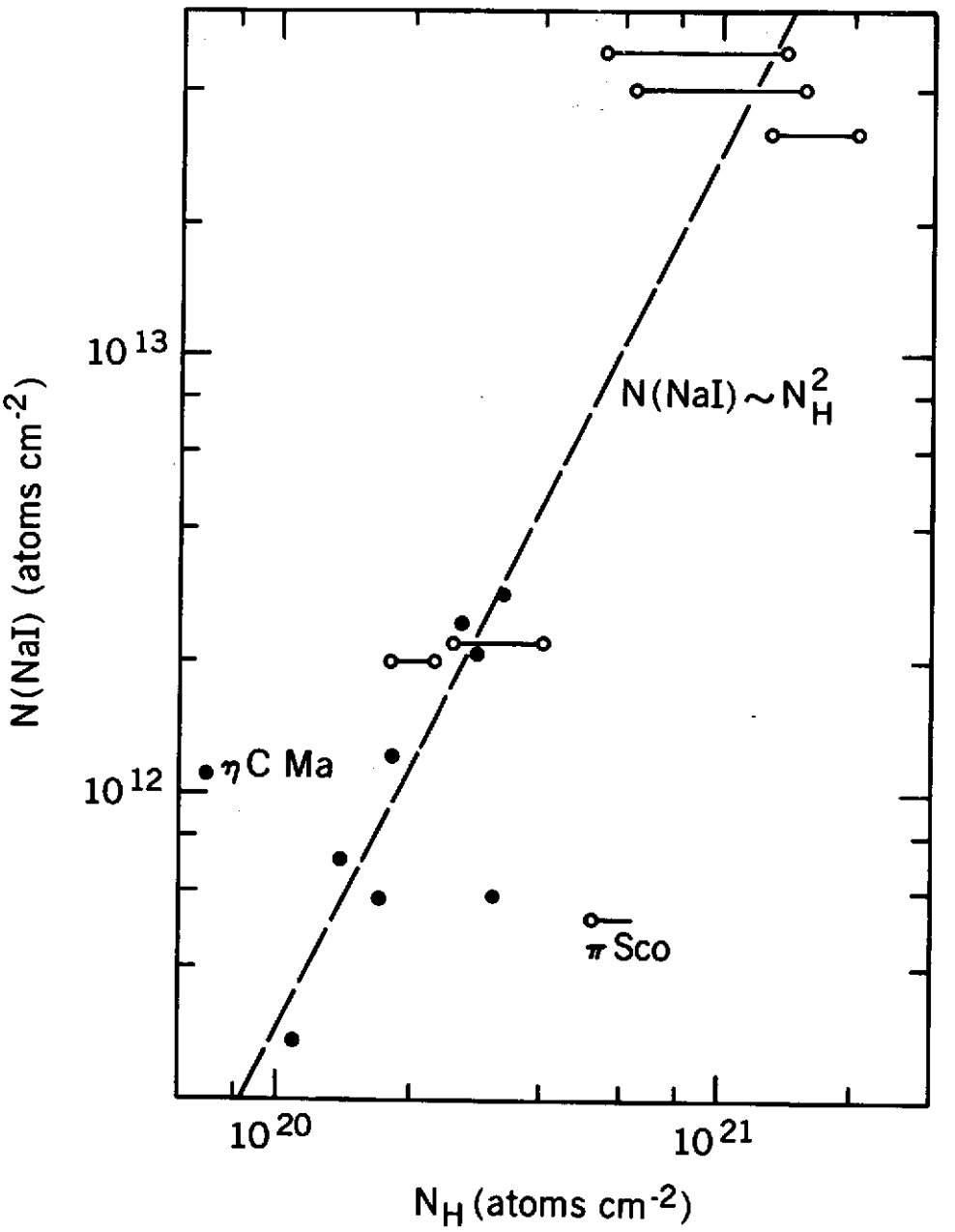
10^{13}
10^{12}
N(NaI) (atoms cm^{-2})
$N(NaI) \sim N_H^2$
ηC Ma
π Sco
10^{20}
10^{21}
N_H (atoms cm^{-2})

FIG. 10